LAWRENCE
LIVERMORE
NATIONAL
LABORATORY

LLNL-TR-684604

The MIDAS touch for Accurately Predicting the Stress-Strain Behavior of Tantalum

S. Jorgensen

March 2, 2016

Disclaimer

This document was prepared as an account of work sponsored by an agency of the United States government. Neither the United States government nor Lawrence Livermore National Security, LLC, nor any of their employees makes any warranty, expressed or implied, or assumes any legal liability or responsibility for the accuracy, completeness, or usefulness of any information, apparatus, product, or process disclosed, or represents that its use would not infringe privately owned rights. Reference herein to any specific commercial product, process, or service by trade name, trademark, manufacturer, or otherwise does not necessarily constitute or imply its endorsement, recommendation, or favoring by the United States government or Lawrence Livermore National Security, LLC. The views and opinions of authors expressed herein do not necessarily state or reflect those of the United States government or Lawrence Livermore National Security, LLC, and shall not be used for advertising or product endorsement purposes.

This work performed under the auspices of the U.S. Department of Energy by Lawrence Livermore National Laboratory under Contract DE-AC52-07NA27344.

The  touch for accurately predicting the stress-strain behavior of tantalum

Shelly Jorgensen

University of Nebraska Lincoln

Research Report for CIVE 498

February 4, 2016

Lawrence Livermore
National Laboratory

This work was performed under the auspices of the U.S. Department of Energy by Lawrence Livermore National Laboratory under Contract DE-AC52-07NA27344

Contents

LIST OF FIGURES

Page

LIST OF TABLES

Page

ABSTRACT

Testing the behavior of metals in extreme environments is not always feasible, so material scientists use models to try and predict the behavior. To achieve accurate results it is necessary to use the appropriate model and material-specific parameters. This research evaluated the performance of six material models available in the MIDAS database [1] to determine at which temperatures and strain-rates they perform best, and to determine to which experimental data their parameters were optimized. Additionally, parameters were optimized for the Johnson-Cook model using experimental data from Lassila et al [2].

INTRODUCTION

Tantalum background

Figure 1: The Falcon Hypersonic Technology Vehicle 2 (HTV-2) utilizes tantalum in its outer shell [3]

Tantalum is an amazing metal with unique properties that make it valuable in the defense, aerospace and biomedical industries. It has an extremely high melting point of 3290 K, which makes it the element with the fifth highest melting point on the periodic table. This attribute makes it ideal for applications such as in nuclear reactors and the HTV-2 (Figure 1), a hypersonic vehicle that reaches speeds of eight times the speed of sound. It is strong and ductile and can be drawn into thin wires, and is often used to make capacitors.

Another useful and unique property of tantalum is that it is biologically inert. Because of this, tantalum is used widely in biomedical applications, such as dental implants and hip replacements. It is also immune to chemical attack below temperatures of 150^{o} C, and at higher temperatures is only susceptible to attack by hydrofluoric acid, acidic solutions containing the fluoride ion, and free sulfur trioxide [4].

MIDAS background

Experimental testing in extreme environments, such as the high temperatures to which tantalum is subjected in the defense industry, is extremely difficult and expensive, so engineers and scientists rely on empirical models to predict how the material will behave.

Material scientists at Lawrence Livermore National Laboratory created a comprehensive materials database called MIDAS (Material Implementation Database and Analysis Source) with information for over 60 different metals and alloys. Each of the metals or alloys has sets of experimental data and constitutive equations designed to model dynamic behavior. Most models have several unique parameter sets—each of them created by optimizing the adjustable parameters to a particular set of experimental data. Tantalum has six material models in MIDAS, 17 unique parameter sets and 59 experimental data sets [1].

Material models

MIDAS has six models for tantalum [1].

- Johnson-Cook (J-C)
- Zerilli-Armstrong (Z-A)
- Preston-Tonks-Wallace (P-T-W)
- Mechanical-Threshold-Stress (M-T-S)
- Steinberg-Guinan (S-G)
- Steinberg-Lund (S-L)

Johnson-Cook [5]

Johnson and Cook developed a model that considers strain-rate and temperature effect on flow-stress. MIDAS includes five unique parameter sets for this model.

$$Y = (A + B\varepsilon^n)(1 + C \cdot \ln\left(\frac{\dot{\varepsilon}}{\dot{\varepsilon_o}}\right)\left(1 - \frac{T - T_{room}}{T_{melt} - T_{room}}\right)^m$$

Where:

- Y = Flow stress (Mbar)
- A = Constant (Mbar)
- B = Constant (Mbar)
- ε = Strain
- n = Hardening exponent
- C = Constant
- $\dot{\varepsilon}$ = Reference strain-rate (μs^{-1})
- $\dot{\varepsilon_o}$ = Normalization factor (μs^{-1})
- T = Reference temperature (K)
- T_{room} = Room temperature (K)
- T_{melt} = Melting temperature (K)
- m = Temperature exponent

Zerilli-Armstrong [6]

Zerilli and Armstrong developed a model for flow stress that considers strain-rate and temperature, as well as an athermal strength which is a function of grain size. MIDAS includes three unique parameter sets for this model.

$$Y = c_0 + c_1 \cdot exp\left[\left(-c_2 + c_3 \cdot \ln\left(\frac{\dot{\varepsilon}}{\dot{\varepsilon_o}}\right)\right)T\right] + c_4 \cdot \exp\left[\left(-c_5 + c_6 \cdot \ln\left(\frac{\dot{\varepsilon}}{\dot{\varepsilon_o}}\right)\right)T\right]\varepsilon^n$$

Where:

- Y = Flow stress (Mbar)
- c_0 = Athermal strength (Mbar)
- c_1 = Leading coefficient for non-hardening term (Mbar)
- c_2 = Thermal only factor for non-hardening term (K^{-1})
- c_3 = Thermal rate factor for non-hardening term (K^{-1})
- $\dot{\varepsilon}$ = Reference strain-rate (μs^{-1})
- $\dot{\varepsilon_o}$ = Normalization factor (μs^{-1})
- T = Temperature (K)
- c_4 = Leading coefficient for hardening term (Mbar)
- c_5 = Thermal only factor for hardening term (K^{-1})
- c_6 = Thermal rate factor for hardening term (K^{-1})
- ε = Strain
- n = Hardening exponent

$$c_0 = \sigma_g + \frac{k}{\sqrt{l}}$$

Where:

c_0 = Athermal strength (Mbar)
σ_g = Athermal strength influence from solute (Mbar)
k = microstructural stress intensity (Mbar·cm)
l = average grain size (cm)

Preston-Tonks-Wallace [7]

The Preston-Tonks-Wallace model was designed to be used in situations modeling explosive loading and high velocity impacts. MIDAS includes only one parameter set for this model.

$$Y = 2\tau^{G(P,T)}$$

$$\hat{\tau} = \hat{\tau}_s + \frac{1}{p}(s_o - \hat{\tau}_y)\ln\left[1 - \left[1 - \exp\left(-p\frac{\hat{\tau}_s - \hat{\tau}_y}{s_o - \hat{\tau}_y}\right)\right]\cdot\exp\left\{-\frac{p\theta\psi}{(s_o - \hat{\tau}_y)\left[\exp\left(p\frac{\hat{\tau}_s - \hat{\tau}_y}{s_o - \hat{\tau}_y}\right) - 1\right]}\right\}\right]$$

$$\text{and } \hat{\tau}_s = s_o - (s_o - s_\infty)\text{erf}\left[k\hat{T}\ln\left(\frac{\gamma\dot{\xi}}{\dot{\psi}}\right)\right]$$

$$\text{and } \hat{\tau}_y = y_o - (y_o - y_\infty)\text{erf}\left[k\hat{T}\ln\left(\frac{\gamma\dot{\xi}}{\dot{\psi}}\right)\right]$$

Where:

Y = Flow stress (Mbar)
$\hat{\tau}$ = Dimensionless stress variable
$\hat{\tau}_s$ = Work hardening saturation stress
p = Hardening rate parameter
s_o = Saturation stress at 0 K
s_∞ = Saturation stress at high temperature
$\hat{\tau}_y$ = Yield stress in thermal activation regime
θ = Initial hardening rate
ψ = Equivalent plastic strain
k = Scale factor for dimensionless temperature
$\hat{T}$= Scaled temperature
γ = Scale factor for strain-rate (s^{-1})
$\dot{\xi}$= Time required for a transverse wave to cross an atom (s)
$\dot{\psi}$ = Scale factor for dimensionless strain-rate
y_o = Yield Strength at 0 K
y_∞ = Yield strength at high temperature

Mechanical-Threshold-Strength [8]

The Mechanical-Threshold-Strength model incorporates mechanical threshold stress, and characterizes it as the sum of the rate-independent dislocation interactions with long-range obstacles, and the rate-dependent interactions with short-range obstacles. It developed from efforts to determine strain in f.c.c. metals at high strain-rates. MIDAS includes two unique parameter sets for this model.

$$Y = \left(\sigma_a + f\left(\bar{\varepsilon}_p, P, T, \hat{\sigma}\right)\right)\frac{G(P,T)}{G_o}$$

$$f\left(\bar{\varepsilon}_p, P, T, \hat{\sigma}\right) = \hat{\sigma}\left\{1 - \left(\log\left(\frac{\dot{\varepsilon}_d}{\dot{\varepsilon}_p}\right)\frac{k}{b^3 g_{od}}\frac{T}{G(P,T)}\right)^{\frac{1}{q_d}}\right\}^{\frac{1}{P_d}} + \hat{\sigma}_i\left\{1 - \left(\log\left(\frac{\dot{\varepsilon}_d}{\dot{\varepsilon}_p}\right)\frac{k}{b^3 g_{oi}}\frac{T}{G(P,T)}\right)^{\frac{1}{q_i}}\right\}^{\frac{1}{P_i}} + \hat{\sigma}_{sol}\left\{1 - \left(\log\left(\frac{\dot{\varepsilon}_d}{\dot{\varepsilon}_p}\right)\frac{k}{b^3 g_{os}}\frac{T}{G(P,T)}\right)^{\frac{1}{q_s}}\right\}^{\frac{1}{P_s}}$$

Where:

Y = Flow stress (Mbar)
σ_a = Athermal contribution to yield stress (Mbar)
$\bar{\varepsilon}_p$ = Mean strain-rate
P = Pressure (Mbar)
T = Temperature (K)
$\hat{\sigma}$ = Threshold stress (Mbar)
G_o = Shear modulus at STP (Mbar)
$\dot{\varepsilon}_d$ = Base strain-rate: dislocation (μs^{-1})
$\dot{\varepsilon}_p$ = Maximum strain-rate (μs^{-1})
k = Boltzmann's constant
b = Burger's vector
g_{od} = Normalized activation energy: dislocation
q_d = Exponential in rate expression: dislocation
P_d = Exponential in rate expression: dislocation
$\hat{\sigma}_i$ = Threshold stress contribution from interstitial (Mbar)
g_{oi} = Normalized activation energy: interstitial
q_i = Exponential in rage expression: interstitial
P_i = Exponential in rate expression: interstitial
$\hat{\sigma}_{sol}$ = Threshold stress contribution from solute (Mbar)
g_{os} = Normalized activation energy: solute
q_s = Exponential in rate expression: solute
P_s = Exponential in rate expression: solute

Steinberg-Guinan [9]

The Steinberg-Guinan model, which accounts for pressure and temperature dependence, work hardening, pressure-dependent melting, Bauschinger effects, strain-rate effects and spall, was developed for high deformation rates. MIDAS includes three unique parameter sets for this model.

$$Y = Y_o[1 + \beta(\varepsilon + \varepsilon_o)]^n \cdot \left[1 + \left(\frac{Y_\rho{}'}{Y_o}\right)\frac{P}{\eta^{\frac{1}{3}}} + \left(\frac{G_T{}'}{G_o}\right)(T - 300)\right]$$

Subject to the limitation that $Y = Y_o[1 + \beta(\varepsilon + \varepsilon_o]^n \leq Y_{max}$

Where:

Y = Flow stress (Mbar)
Y_0 = Yield strength at Hugoniot elastic limit (Mbar)
β = Work hardening parameter
ε = Strain
ε_o = Initial plastic strain
n = Work hardening exponent
$Y_P{}'$ = Stress at pressure P (Mbar)
P = Pressure (Mbar)
η = Compression
$G_T{}'$ = Shear modulus at temperature T (Mbar)
G_o = Shear modulus at STP (Mbar)
T = Temperature (K)
Y_{max} = Work hardening maximum (Mbar)

Steinberg-Lund [10]

The Steinberg-Lund model was developed to model strain rates from 10^{-4} to 10^6 s^{-1}, expanding and improving on the original model developed by Steinberg and Guinan. MIDAS includes three unique parameter sets for this model.

$$Y = \left[Y_T(\dot{\varepsilon}, T) + Y_A(\varepsilon_p)\right] G(P, T) G_o$$

Subject to constraints that $Y_A(\varepsilon_p) = Y_A[1 + \beta(\varepsilon + \varepsilon_o)]^n \leq Y_{max}$

$$\text{and} \quad \dot{\varepsilon} = \left\{ \frac{1}{c_1} \exp\left[\frac{2U_k}{kT} \left(1 - \frac{Y_T}{Y_P} \right)^2 \right] + \frac{C_2}{Y_T} \right\}$$

$$\text{and } Y_T \leq Y^*_{max}$$

Where:

Y = Flow stress (Mbar)	ε = Strain
Y_T = Thermally activated part of yield stress	ε_o = Initial plastic strain
$\dot{\varepsilon}$ = Reference strain rate (μs^{-1})	n = Work hardening exponent
T = Temperature (K)	Y_{max} = Work hardening maximum (Mbar)
Y_A = Athermal yield strength (Mbar)	C_1 = Reference strain-rate in thermal activation regime (μs^{-1})
ε_p = Equivalent plastic strain	$2U_k/k$ = Activation energy over Boltzmann constant (eV)
P = Pressure	Y_P = Peierls stress (Mbar)
G_o = Shear modulus at STP	C_2 = Coefficient in the drag regime (Mbar·μs)
β = Work hardening parameter	Y^*_{max} = Work hardening max for rate-dependent term (Mbar)

Experimental data sets

All 59 experimental data sets available on MIDAS for tantalum [1] were used to determine where the models performed best and to which experimental data the model parameters had been fit. The temperatures for these data sets ranged from 77 K to 1273 K and the strain-rates ranged from 1.6 x 10^{-11} μs^{-1} to 8.0 x 10^{-3} μs^{-1}.

Experimental data sets from Lassila et al [2] were used to optimize the Johnson-Cook material model parameters. There were two strain-rates for this data: 1 x 10^{-10} s^{-1} and 1 x 10^{-7} s^{-1}, covering temperatures of 150, 200, 250, 300, 400, 573, 723 and 900 K.

Determining strain-rates and temperatures where models performed best

MIDAS [1] has the ability to create a stress-strain plot for a material, based on the model and the parameters, and to then compare that plot to a set of experimental data with the same temperature and strain-rate. The average percent error for the entire curve is calculated by summing the discrete percent errors and dividing by the total number of points (n), as shown in the equation below.

$$Average\ \%\ error = \frac{\sum_1^n \frac{Y_{model} - Y_{experimental}}{Y_{experimental}}}{n} (100\%)$$

Where:

Y_{model} = stress value calculated by model (Mbar)
$Y_{experimental}$ = stress value of experimental data (Mbar)
n = total number of points

Using the temperature and strain-rate from each of the 59 tantalum experimental data sets in MIDAS [1], a plot was created with the six material models and their unique parameter sets. The model plots were then compared to the corresponding experimental data and percent error was calculated.

The percent error data was compiled, organized and analyzed to determine at which temperatures and strain-rates the models performed best. By creating individual spreadsheets with percent error sorted according to strain-rate and temperature, it was possible to see where the models performed well.

Performing "well" was an arbitrary determination based on personal experience of the author with optimizing material models, and the broad range of percent error results for this research. A cut-off of 17% was used to define performing well because the author found that getting less than a 17% average error was challenging. Choosing a lower cut-off point would have excluded many of the models.

Determining which data sets were used to develop parameter sets in MIDAS

In order to determine which experimental data was used to develop the parameter sets in MIDAS, the percent error data was sorted based on the author(s) of the experimental data. It was possible to see that certain sets of experimental data (by a specific author) tended to have lower percent errors. The graphs were also compared visually to compare curve shapes. By knowing which experimental data set was used, it is possible to evaluate additional information about the specific tantalum sample used, which could be helpful for developing future model equations.

Optimizing parameters for the Johnson-Cook model

Optimization of the Johnson-Cook model was accomplished by adjusting the parameters *A, B, C, n* and *m* and comparing the curve-fit to experimental data. Improvement was gauged objectively by comparing percent error, and subjectively by visually evaluating the curve-fit. During the optimization process it was noted that it was much more difficult to improve the percent error at temperatures below 300 K. Because of this, a set of parameters was optimized for the "low" temperatures (150-250 K) and for the "high" temperatures (300-900 K), before optimizing the full set.

To adjust the parameters and improve the curve fit, an understanding of the Johnson-Cook model is useful. The equation has three basic segments, set apart parenthetically, that are multiplied together. The paragraphs below describe how the adjusting the parameters affects the shape of the curve.

The first segment, $(A + B\varepsilon^n)$, is the equation of a parabola. For illustration, Figures 2, 3 and 4 use Y = 0 + 1·x ^{½} as the reference plot. This segment of the equation represents the yield stress of the material (*A*) added to the effect of hardening (*B*) as a component of strain (*n*). Increasing or decreasing *A* shifts the parabola up or down vertically (Figure 2). Decreasing *B* moves the curve down, while increasing *B* increases the height of the curve (Figure 3). Increasing *n* has a more dramatic effect on the shape and steepness of the curve at larger strains (Figure 4).

The second segment of the Johnson-Cook model equation, $\left(1 + C \cdot \ln\left(\frac{\dot{\varepsilon}}{\dot{\varepsilon_o}}\right)\right)$, represents the influence of strain-rate, where $\dot{\varepsilon}$ is the reference strain-rate and $\dot{\varepsilon_o}$ is the normalization factor (10^{-6} μs^{-1} in this case). If this segment of the Johnson-Cook model represents a percentage of the influence strain-rate has on strength, 100% would show that the material retains equivalent strength, over 100% would mean it is increasing in strength, and a percentage lower than 100% would show a decrease in strength, all based on the applied strain-rate. Strain-rates faster than the normalization rate give a higher predicted strength, representative of deformation mechanisms that require higher stress levels to operate.

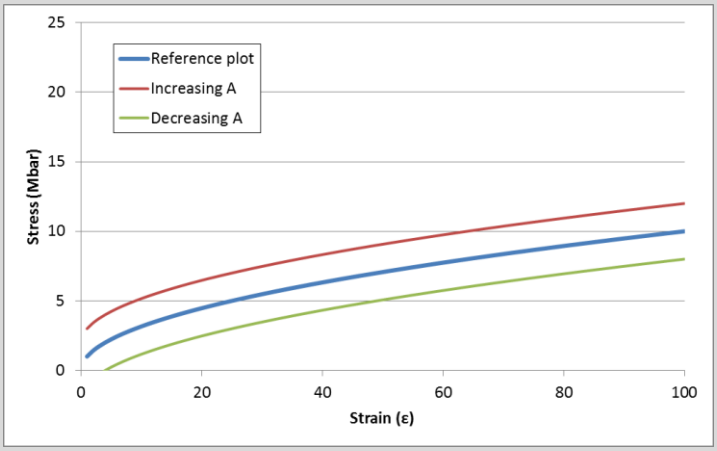

Figure 2: Effect of increasing or decreasing parameter *A* by 2.0 on $y = (A + B\varepsilon^n)$ when *B* = 1, *n* = 0.5

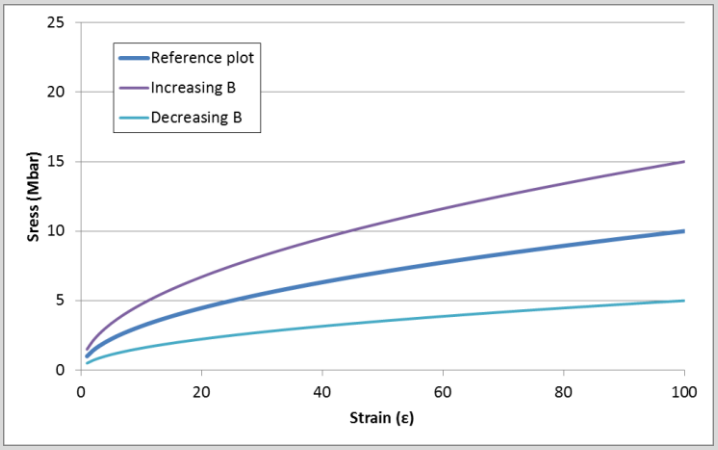

Figure 3: Effect of increasing or decreasing parameter *B* by 0.5 on $y = (A + B\varepsilon^n)$ when *A* = 0, *n* = 0.5

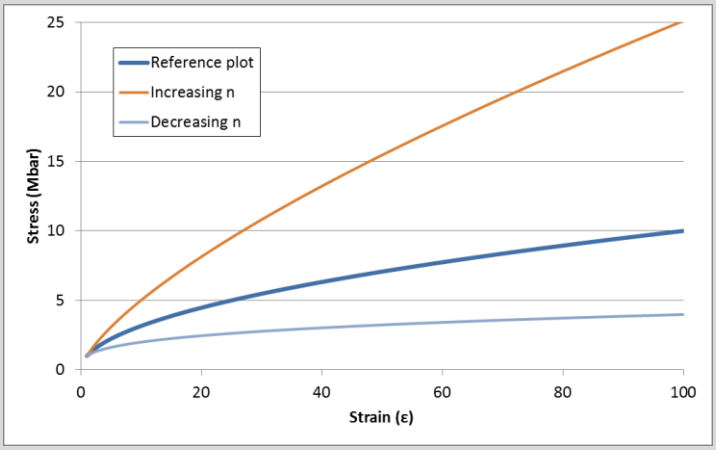

Figure 4: Effect of increasing or decreasing parameter *n* by 0.2 on $y = (A + B\varepsilon^n)$ when *A* = 0, *B* = 1

Depending on the strain-rate, adjusting parameter *C* requires a different thought process. If the reference strain-rate is higher than the normalization factor, the natural log is positive, and an increasing *C* magnifies the hardening effect (Figure 5). If the reference strain-rate is lower than the normalization factor, the natural log of that number is less than zero, so unless *C* is a negative number, which is not usually the case, an increasing *C* amplifies strain-softening (Figure 6), shifting the stress-strain curve down.

With higher strain-rates, decreasing *C* moves the stress-strain curve down (Figure 5). Conversely, with low strain-rates, decreasing *C* moves the curve up (Figure 6).

The variable *C* controls strain-rate sensitivity. Regardless of reference strain-rate, a smaller *C* value diminishes the effect of strain-rate, and a higher value for *C* makes the equation more sensitive to strain-rate effects.

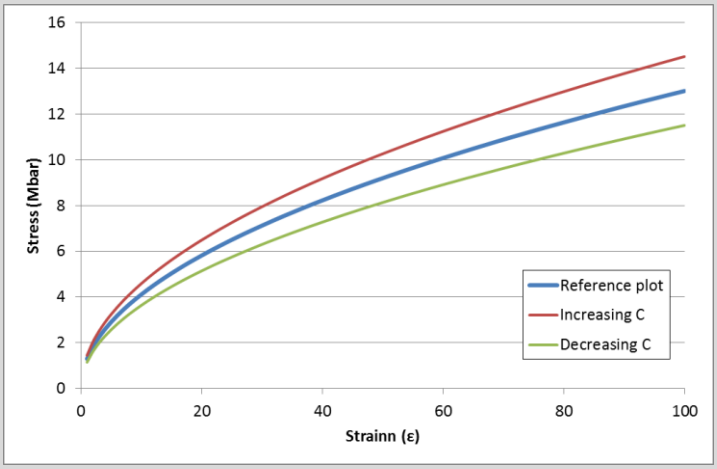

Figure 5: Effect of increasing or decreasing parameter *C* by 0.5 when strain-rate is higher on $y = (A + B\varepsilon^n)\left(1 + C \cdot \ln\left(\frac{\dot{\varepsilon}}{\dot{\varepsilon_o}}\right)\right)$ when $A = 0$, $B = 1$, $n = 0.5$, $\dot{\varepsilon} = 2$, $\dot{\varepsilon_o} = 1$, $C = 1$)

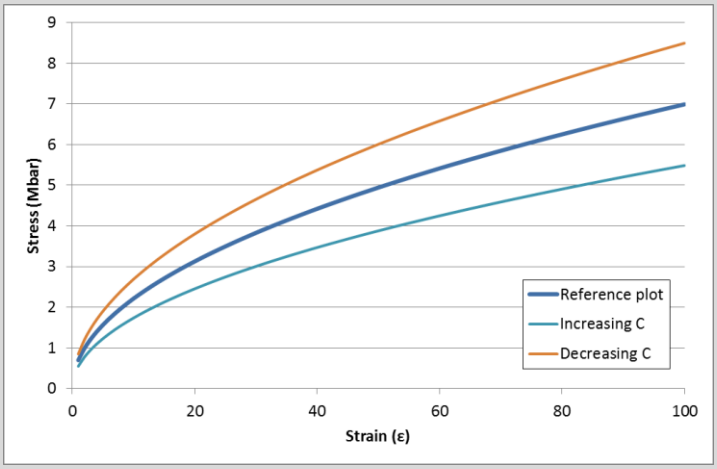

Figure 6: Effect of increasing or decreasing parameter *C* by 0.5 when strain-rate is lower on $y = (A + B\varepsilon^n)\left(1 + C \cdot \ln\left(\frac{\dot{\varepsilon}}{\dot{\varepsilon_o}}\right)\right)$ when $A = 0$, $B = 1$, $n = 0.5$, $\dot{\varepsilon} = 0.5$, $\dot{\varepsilon_o} = 1$, $C = 1$)

The last segment of the equation, $\left(1 - \frac{T - T_{room}}{T_{melt} - T_{room}}\right)^m$, factors in the influence of temperature on strength. It is obvious that when most materials are warmer, they soften. At room temperature, the temperature effect is zero, reducing this segment to $(1)^m$. High temperatures result in a larger temperature effect, which when subtracted from one leaves a smaller multiplier $(<1)^m$. For high temperatures, increasing *m* lowers the curve and decreasing *m* raises the curve (Figure 7).

For temperatures less than room temperature, the temperature effect is positive $(>1)^m$, and increasing *m* raises the curve, while decreasing *m* lowers the curve (Figure 8).

When optimizing the model parameters to fit experimental data, the effects are inter-connected, complicating the process.

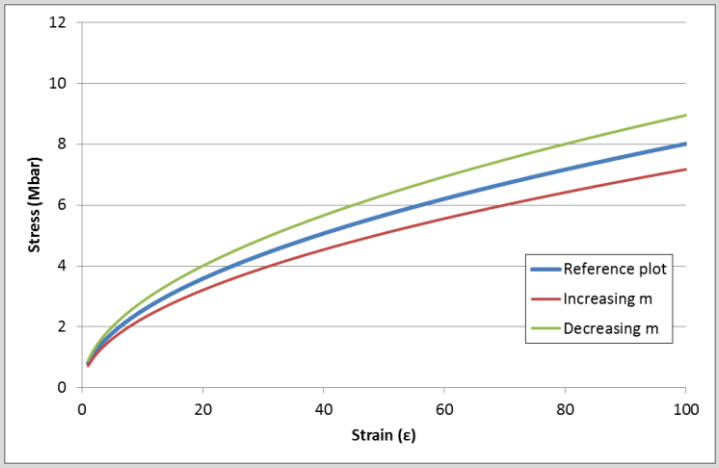

Figure 7: Effect of increasing or decreasing parameter *m* by 0.5 when temperature is higher than room temperature on $y = (A + B\varepsilon^n)\left(1 + C \cdot \ln\left(\frac{\dot{\varepsilon}}{\dot{\varepsilon_o}}\right)\right)\left(1 - \frac{T - T_{room}}{T_{melt} - T_{room}}\right)^m$ when A = 0, B = 1, n = 0.5, $\dot{\varepsilon}$ = 0.5, $\dot{\varepsilon_o}$ = 1, C = 1, T_{room} = 294 K, T_{melt} = 3290 K and T = 900 K

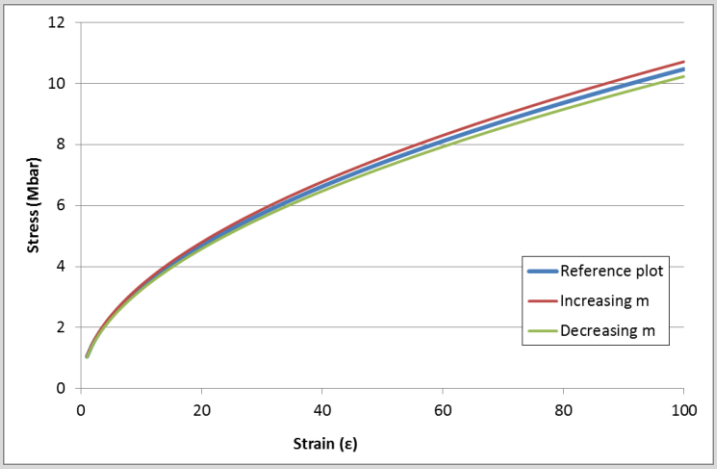

Figure 8: Effect of increasing or decreasing parameter *m* by 0.5 when temperature is lower than room temperature on $y = (A + B\varepsilon^n)\left(1 + C \cdot \ln\left(\frac{\dot{\varepsilon}}{\dot{\varepsilon_o}}\right)\right)\left(1 - \frac{T - T_{room}}{T_{melt} - T_{room}}\right)^m$ when A = 0, B = 1, n = 0.5, $\dot{\varepsilon}$ = 0.5, $\dot{\varepsilon_o}$ = 1, C = 1, T_{room} = 294 K, T_{melt} = 3290 K and T = 150 K

Strain-rates and temperatures where models performed best

The colored bars in Figure 9 indicate at what temperatures and strain-rates the models consistently had less than a 17% average error for the 59 experimental data sets in MIDAS using the 17 unique parameter sets available. The table shows only the 10 parameter sets that performed well.

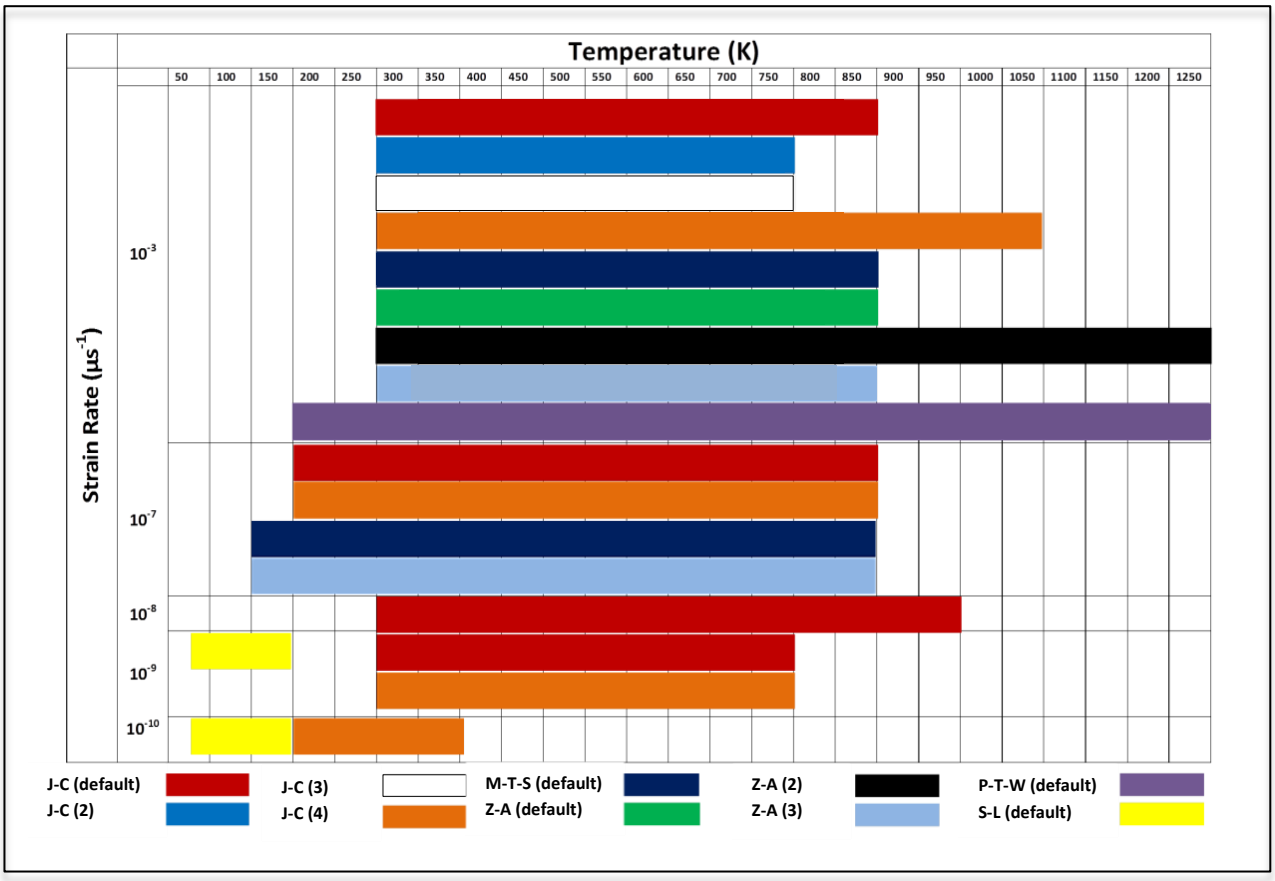

Figure 9: Strain-rates and temperature ranges at which models performed best (<17% average error)

Many parameter sets performed well in the 10^{-3} μs^{-1} range, and fewer parameter sets performed well at lower strain-rates. Of the ten parameters sets in Figure 9, only two parameter sets, both of which are for the Johnson-Cook model, perform well at both low and high strain-rates.

Parameter sets in the 10^{-3} μs^{-1} range were more accurate above 200 K. In the very low temperature range, only one model (Steinburg-Lund) was able to predict the stress-strain behavior with less than a 17% error, and only at low strain-rates. Only two parameter sets excelled at temperatures above 1100 K; Zerilli-Armstrong (2) and Preston-Tonks-Wallace (default).

The Johnson-Cook model was able to predict the behavior of tantalum with less error at high temperatures than at lower temperatures, because it does not model the spike that occurs at low temperatures, as shown in Figure 10.

Data sets used to fit parameters

By noting which of the 59 experimental data sets in MIDAS had the lowest percent error for each unique parameter set, it was apparent which experimental data was used to develop them. Table 1 shows the experimental data set used to fit each of the 10 parameter sets that performed well.

Table 1: Data sets used to determine parameters for various material models

Material Model	Parameter Set [1]	Data Set Author(s)	Data Set Strain-Rate (μs^{-1})
Johnson-Cook	Default	Chen-Grey	10^{-3}
Johnson-Cook	(2)	Nemat-Nasser	10^{-3}
Johnson-Cook	(3)	Nemat-Nasser	10^{-3}
Johnson-Cook	(4)	Perez	10^{-3}
Zerilli-Armstrong	Default	Nemat-Nasser	10^{-3}
Zerilli-Armstrong	(2)	Chen-Grey	10^{-3}
Zerilli-Armstrong	(3)	Nemat-Nasser	10^{-3}
Mechanical-Threshold-Stress	Default	Lassila	10^{-7}
Preston-Tonks-Wallace	Default	Chen-Grey	10^{-3}
Steinburg-Lund	(2)	Lassila	10^{-3}

All but one of the models were fit to experimental data with strain-rates in the range of 10^{-3} μs^{-1}. The models should perform best at strain-rates near that of the experimental data to which they were fit. It is interesting to note that some of these versions fortuitously predicted the slower strain-rate data accurately.

Optimized parameters

Using a set of experimental data from Lassila et al [2] and carefully adjusting the parameters, as described in the methods section, it was possible to increase the accuracy of the Johnson-Cook model, as compared to using the default values. Table 2 shows the values of the optimized and default parameters and the average percent error for each.

Table 2: Johnson-Cook parameter values used in the optimization process

Parameter Set	A (Mbar)	B (Mbar)	C	m	n	Average Error
Full set—Default	0.0034	0.0075	0.0575	0.4000	0.7000	32.6%
Full set—Optimized	0.0018	0.0075	0.0213	0.3773	0.4215	15.1%
Low temp (150-250 K)—Default	0.0034	0.0075	0.0575	0.4000	0.7000	43.3%
Low temp (150-250 K)—Optimized	0.0025	0.0050	0.0300	0.3000	0.3000	18.7%
High temp (300-900 K)--Default	0.0034	0.0075	0.0575	0.4000	0.7000	31.0%
High temp (300-900 K)—Optimized	0.0015	0.0075	0.0246	0.4500	0.4500	9.6%

Comparison between the average percent error for the default parameters and the optimized parameters shows a drastic improvement for the optimized parameters—116% improvement for the full set, 134% for the low temperature range and 223% for the high temperature range. This makes sense because the Johnson-Cook default parameters were fit to Chen & Grey [1] experimental data, not Lassila et al experimental data [2].

The accuracy attained for the optimized parameters in the higher temperature range (300-900 K), was much better than for the lower temperature range (150-200 K)—a 9.6% average error as compared to 18.7% average error, respectively. The average percent error for the full set was 15.1%. The full set percent error appears to be strongly influenced by the model's inability to model the low temperature range. The optimized parameter set works better in the higher temperature range, as can be seen best in Figure 11, where the lower model plots (high temperatures) fit the experimental data much better than the upper model plots (low temperatures).

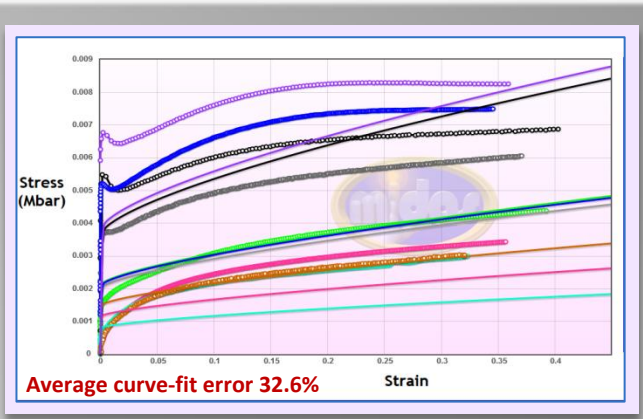

Figure 10: Plot of experimental data vs. J-C model using default parameters, full set

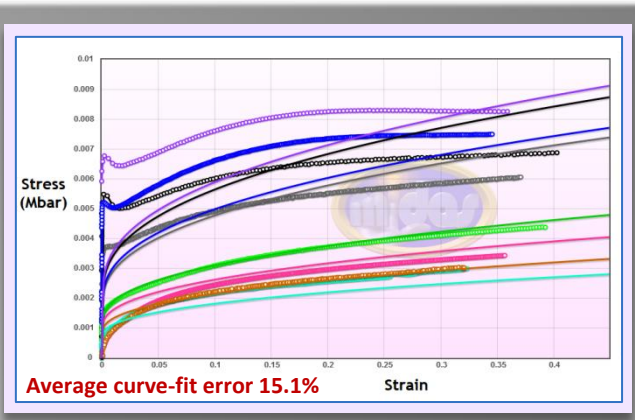

Figure 11: Plot of experimental data vs. J-C model with parameters optimized, full set

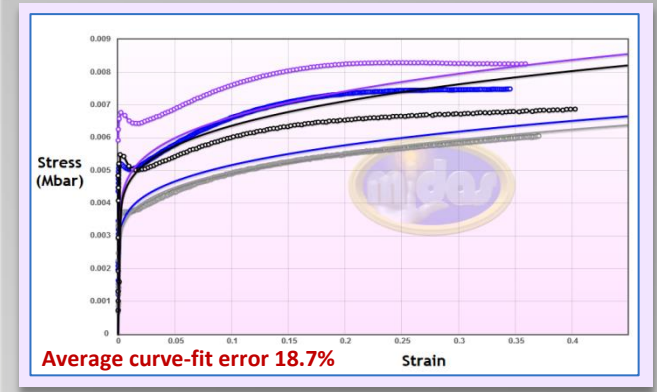

Figure 12: Plot of experimental data vs. JC model with parameters optimized, low temp (150-250 K)

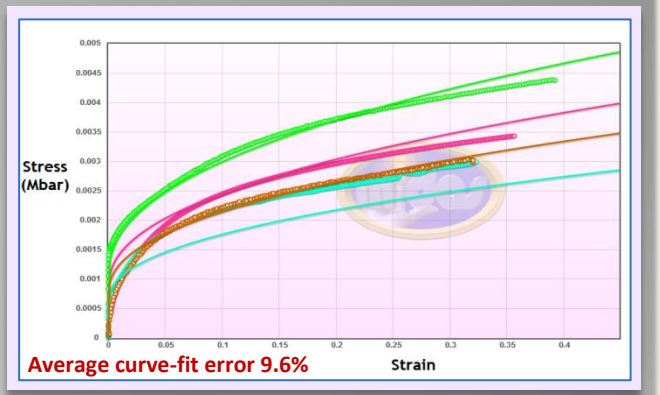

Figure 13: Plot of experimental data vs. J-C model with parameters optimized, high temp (300-900 K)

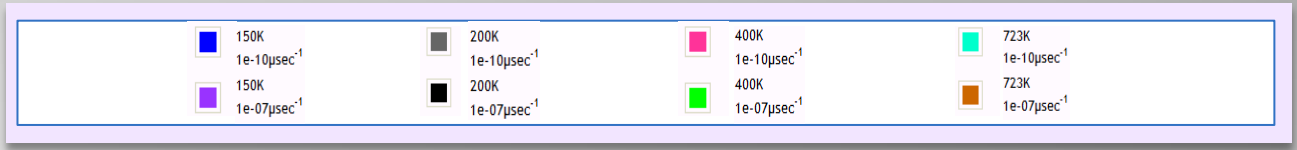

Thin lines represent model plots and the thicker, dotted lines represent experimental data plots.

The Johnson-Cook equation models a simple parabolic curve, as explained in the methods section, and as a result it does not contain the necessary physics to predict the initial spike in stress that occurs due to limits on the ability of the dislocations to accommodate the initial strain at higher strain-rates and lower temperatures. Figures 10, 11, and 12 clearly show the spike is largest at low temperatures. The higher temperature data sets do not have the spike because hot metal is softer, and the deformation mechanisms can easily accommodate the strain under these conditions. The similarity in curve shape between the high temperature data and the Johnson-Cook model equation decreases the percent error in the high temperature range.

CONCLUSION

Of the 17 parameter sets analyzed, 10 were able to predict stress-strain behavior with an average percent error of less than 17% within specific strain-rate and temperature ranges. The Johnson-Cook model performed well over a greater temperature and strain-rate range than the other material models. Only the Steinberg-Lund model performed well at low strain-rates and low temperatures. All but one of the parameter sets analyzed appear to be fit to experimental data with a strain-rate in the range of 10^{-3} μs^{-1}.

A parameter set was optimized using the Johnson-Cook model and Lassila et al [2] experimental data. As would be expected, the optimized parameters predicted the stress-strain values of the experimental data more accurately than the default parameters. Modeling the low temperature range data accurately was much more difficult than the higher temperature range data. It was concluded that the Johnson-Cook model does not have the physics necessary to accurately predict stress-strain behavior at lower temperatures.

ACKNOWLEDGEMENTS

Special thanks to Jeffrey Florando, Nathan Barton, Peter Norquist, Kevin Durrenberger, Ilya Golosker, Jessica Williams and Bert Jorgensen for their contributions to this research.

REFERENCES

1) Barton, N., Florando, J., Durrenberger, K., and P. Norquist. MIDAS. Computer software. MIDAS. Vers. 1.2. Lawrence Livermore National Laboratory, n.d. Web. July 2015.
2) Lassila, D.H., Goldberg, A., and R. Becker. "The effect of grain boundaries on the athermal stress of tantalum and tantalum-tungsten alloys." Mellallurgical and Materials Transactions A, November 2002.
3) Shachtman, N. "Pentagon's Mach 20 Missile Lost Over Pacific — Again." Wired.com. Conde Nast Digital, 11 Aug 2011, Web. 24 July 2015.
4) "Periodic Table of Elements: Los Alamos National Laboratory." Periodic Table of Elements: Los Alamos National Laboratory. Los Alamos National Security, LLC, Web. 29 July 2015.
5) Johnson, G.R., and W.H. Cook. "A Constitutive Model and Data for Metals Subjected to Large Strains, High Strain-rates and High Temperatures." *Proceedings of the 7th International Symposium on Ballistics* (1983): 541-48. Print.
6) Zerilli, F.J., and R.W. Armstrong. "Dislocation-mechanics-based Constitutive Relations for Material Dynamics Calculations." *J. Appl. Phys. Journal of Applied Physics* 61.5 (1987): 1816-825. Print.
7) Preston, D.L., Tonks, D.L., and D.C. Wallace. "Model of Plastic Deformation for Extreme Loading Conditions." *J. Appl. Phys. Journal of Applied Physics* 93.1 (2003): 211-20. Print.
8) Follansbee, P.S., and U.F. Kocks. "A Constitutive Description of the Deformation of Copper Based on the Use of the Mechanical Threshold Stress as an Internal State Variable." *Acta Metallurgica* 36.1 (1988): 81-93. Print.
9) Steinberg, D.J., Cochran, S.G., and M.W. Guinan. "A Constitutive Model for Metals Applicable at High-strain Rate." *J. Appl. Phys. Journal of Applied Physics* 51.3 (1980): 1498-1504. Print.
10) Steinberg, D.J., and C.M. Lund. "A Constitutive Model for Strain-rates from 10^{-4} to 10^{6} S^{-1}." *J. Appl. Phys. Journal of Applied Physics* 65.4 (1989): 1528-533. Web.